GSI

REPORT 98-03
Februar 1998

Optimal Shaping: Advanced Version
- Aspherical Lens Design -

L. G. Vorobiev, R. W. Müller

Gesellschaft für Schwerionenforschung mbH
Planckstraße 1 • D-64291 Darmstadt • Germany
Postfach 11 05 52 • D-64220 Darmstadt • Germany

Optimal Shaping: Advanced Version
— Aspherical Lens Design —

L.G. Vorobiev[a,1], and R.W. Müller[b]

[a] Institute of Theoretical and Experimental Physics (ITEP), Moscow 117259, Russia

[b] Gesellschaft für Schwerionenforschung mbH, GSI, D-64220 Darmstadt

Abstract

The shaping algorithm, introduced in [1], was developed further and applied to design high-performance aspherical lenses for light optics.

1 Introduction

In this paper we develop further the "shaping algorithm", introduced in [1]. As before, we shall interpret "the shaping" as a search for a continuous function (the so-called "goal-function") which provides an extremum of the optimization criterion and satisfies boundary constraints. In this advanced version the boundary constraints may either be fixed or may vary during shaping, depending on the actual problem to be solved.

We will systematize our method and broaden its application for light optics. A search for "non-standard" geometry for optics design is a challenging idea. In this paper we give a few examples of high-performance glass lenses, designed by our algorithm. These multi-functional lenses with aspherical surfaces will have much more better optical characteristics than spherical ones, especially for full aperture beams [2, 3].

2 New Features of the Shaping Algorithm

A detailed computational scheme of the shaping algorithm was described in [1]. The optimal shaping was formulated in terms of a constrained variational problem, whose solution should represent a function $\mathrm{F}(s)$ minimizing a quantitative criterion $\Phi(\mathrm{F}(s))$ and satisfying additional boundary conditions:

$$\Phi(\mathrm{F}(s)) \to \min \qquad (1)$$

subject to:

[1] e-mail: lgvor@vitep5.itep.ru

$$\begin{cases} F(\tilde{s}_0) = \mathcal{F}_0 & F(\tilde{s}_1) = \mathcal{F}_1 \\ F'(\tilde{s}_0) = \mathcal{F}'_0 & F'(\tilde{s}_1) = \mathcal{F}'_1 \\ \vdots & \vdots \\ F^{(p)}(\tilde{s}_0) = \mathcal{F}_0^{(p)} & F^{(p)}(\tilde{s}_1) = \mathcal{F}_1^{(p)} \\ p = 0, 1, \ldots P & \end{cases} \tag{2}$$

where the function $F(s)$ varied within an interval $[\tilde{s}_0, \tilde{s}_1]$ ($\tilde{s} = \tilde{s}_1 - \tilde{s}_0$ is its length) and $F^{(p)} = d^p F / ds^p$. The set of conditions (2) define the function values $\mathcal{F}_{0,1}$ and derivatives $\mathcal{F}_{0,1}^{(p)}$ on the boundary.

A numerical method to solve the problem (1)-(2) was based on the Ritz approach [4], which was reduced then to a constrained gradient minimization. Our optimizer worked well with arbitrary boundary constraints, even with singular ones, as it was shown in [1].

During further numerical experiments we faced some situations when the convergence of the minimization process became slower and/or the minimum was not achieved at all. It necessitated further developments and improvement of the algorithm.

Split of the shape function. An effective way to increase a flexibility of the computational scheme, introduced in [1] to solve (1)-(2), is to split the original function $F(s) = F_{var}(s) + F_{back}(s)$, where

$$\begin{cases} F_{var}(\tilde{s}_0) = 0 & F_{var}(\tilde{s}_1) = 0 \\ F_{var}^{(p)}(\tilde{s}_0) = 0 & F_{var}^{(p)}(\tilde{s}_1) = 0 \end{cases} \tag{3}$$

and

$$\begin{cases} F_{back}(\tilde{s}_0) = \mathcal{F}_0 & F_{back}(\tilde{s}_1) = \mathcal{F}_1 \\ F_{back}^{(p)}(\tilde{s}_0) = \mathcal{F}_0^{(p)} & F_{back}^{(p)}(\tilde{s}_1) = \mathcal{F}_1^{(p)} \end{cases} \tag{4}$$

with $p = 0, 1, \ldots P$. The function $F_{back}(s)$ represents now the "background function", satisfying the boundary constraints, does not vary during shaping, while $F_{var}(s)$ does. An appropriate split may significantly accelerate the convergence to the solution (see ref.[5]).

The solution of the auxiliary problem (1), (3-4) may be found by the regular procedure from [1], when the Fourier series will include only even harmonics.

The convergence of minimization can be very high due to "non-steep behavior" of F(s), whereas the "background function" F_{back}, responsible for non-zero boundary, could have a very special behavior, even with a singular boundary (see for details [1, 5, 6].

In the simplest case there are only four constraints: $\mathcal{F}_0$, $\mathcal{F}_1$, $\mathcal{F}'_0$, $\mathcal{F}'_1$, and the background function $F_{back}(s)$ therefore can be represented by a cubic polynomial. For many practical situations these four constraints are quite sufficient.

Matching of Boundary Constraints. As a result of such a split representation of $F(s)$ we could manage very special boundary limitations and, what is also important, it helps to come to a new understanding of the original variational problem.

Until now we were considering the frozen boundary limitations. In the meantime the choice of these constraints is not trivial, excepting those cases when they are well-defined a priori or there is a mandatory demand to satisfy certain limitations known beforehand. However, if the initial assignment of $\mathcal{F}_{0,1}^{(p)}$ is too rough, the solution can not be found at all. Numerical studies showed us that if this boundary set would be changed even slightly, we could succeed in searching for the better solutions.

We had to develop further our algorithm for the situation with released edges, which presents a more general case of constrained optimization [4, 7]. We assume now that the boundary constraints $\mathcal{F}_{0,1}^{(p)}$, etc. are not permanently fixed anymore: they can be "de-frozen" and corrected in a proper way.

The manual selection of the appropriate boundary parameters is too slow and is acceptable only for simple situations, when we fit the boundary set every time before the shaping session. Our computer program releases the boundary during the shaping and matches them automatically. Technically this idea was realized via the abovementioned split of the original function, where F_{back} is responsible for the constraints and F_{var} is used to do "the fine" tuning.

There are two steps in the current version of the optimization subroutine: an internal block, which performs the shaping within strictly fixed boundary, tuning F_{var}, and an external loop which optimally varies the "background function" F_{back}, matching the set of constraints. The switch from internal block to external loop, then back to internal block and so on, helps to pass local minima, finding the global minimum of the criterion $\Phi(F)$, i.e. the very best solution of the problem. Note that the matching of $\mathcal{F}_{0,1}^{(p)}$ can be selective: either all this set is being matched or only a subset (e.g. only one edge can be released, only coordinates, only derivatives, etc.).

In the examples below this technique was used quite often and rather successfully that gives us confidence to recommend it especially for those situations where the boundaries are not well-established prior to the design.

3 Design of Aspherical Lenses for Light Optics.

Spherical lenses are widely used in light optics and have the advantages that the fabrication and control of spherical surfaces are rather easy to provide. Another circumstance, which facilitates a theoretical analysis and practical design of optical systems, is that high order aberrations for these lenses are expressed by the same universal formulae. However, some imperfections of spherical lenses are inevitable and deteriorate the quality of focusing especially when using non-paraxial large aperture ratio and/or inclined off-axis beams. As a result well-known aberrations arise, such as astigmatism, coma, spherical aberrations, distortions and field curvature [2, 8].

A possible way to upgrade parameters of optical devices is to use aspherical lenses [2, 3, 9]. Application of these lenses becomes very important if we build objectives with large relative and angular apertures, increased brightness, sharpness and extreme resolving power. The aspherical surfaces also help to reduce the number of lenses, that gives an additional gain and is especially attractive for portable devices (best brands of cameras often use such high-performance lenses). Note, that hystorically the idea of non-spherical glass surfaces originates from Descartes and Huygens [10], who had studied some features of aspherical lenses and derived analytical formulae for their surfaces.

Nowadays, the optimization of optical systems uses widely computer methods. A possible computational approach to find optimal lens surface can be formulated as a solution of our variational problem (1)-(2), and our "shaping" algorithm will eliminate spherical, 5-th and higher order aberrations, distortion, coma and dispersion. Optimal surfaces of lenses will be found in frames of geometrical ray optics, based on the Fermat's principle of least time.

The refraction law, realized in the computational block of ray tracing, gives a relation between the angle of incidence γ_1 and the angle of refraction γ_2 according to the refraction law:

$$\frac{\sin\gamma_1}{\sin\gamma_2} = n_{21}$$

where the coefficient n_{21} stands for the refraction factor (for glass lenses this coefficient is about of $n_{21} \approx 1.5 - 1.65$). When the lens thickness is relatively in comparison with its size, there is a relation between the image distance $\mathbf{L}^{image}$ and the object distance $\mathbf{L}^{obiect}$:

$$\frac{1}{\mathbf{L}^{image} - D_1} - \frac{1}{\mathbf{L}^{object} - D_2} = (n_{21} - 1)(\frac{1}{R_1} - \frac{1}{R_2}) \tag{5}$$

where $R_{1,2}$ are curvature radii and $D_{1,2}$ are thickness' of the lens from the corresponding surfaces to the center. All rays are paraxial. This model is the so-called "thin lens approximation".

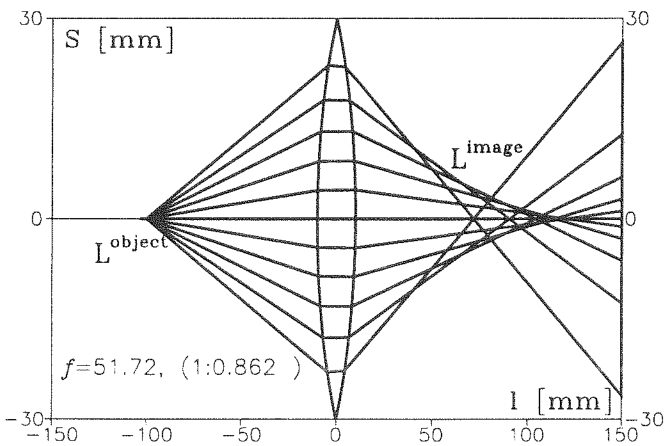

Figure 1: Illustration of spherical aberrations: a bunch of rays $x_r(l)$ (r=1,...,10) passes through a spherical lens, whose aperture ratio is of $\emptyset : f$=1:0.862.

Let us consider a symmetrical spherical lens (with both radii $|R_{1,2}|$=50 mm) and with a diameter $\emptyset = 60$ mm, whose surfaces are described by the shape function $\mathrm{F}_{sph}(s)$:

$$s^2 + (\mathrm{F}_{sph}(s) \pm 40)^2 = R_{1,2}^2$$

Substituting in the formula (5) R_1 =50 mm, R_2 =-50 mm, $\mathbf{L}^{object}$=-100 mm, $D_{1,2}$=10 mm and assuming the refraction factor $n_{21} = 1.50$ (close to a refraction index of a usual glass), we find that the image distance must be equal to $\mathbf{L}^{image}$=122.5 mm.

The principal focus f of such a spherical lens can be found by

$$f = \frac{n_{21} R_1 R_2}{(n_{21}-1)[n_{21}(R_2-R_1)+(n_{21}-1)D]} \tag{6}$$

and is equal f=51.72 mm; the relative aperture ratio therefore is of $\emptyset : f$=1:0.862, that is rather extreme.

In Fig. 1 a result of numerical simulation is shown: N^{rays} rays, ejected from the object point $(0, \mathbf{L}^{object})$, pass through the spherical lens: paraxial rays have a fine focus in the point $\mathbf{L}^{image} = 122.5$ mm, that coincides pretty well with the analytical result. The quality of non-paraxial focusing, however, is spoiled, that illustrates the well known effect of spherical aberrations, relevant to any spherical lens.

Elimination of Spherical and Higher Order Aberrations by Lenses Shaping. Now we apply the "shaping algorithm" to find aspherical lenses with improved focusing properties. The coordinate and slope of every ray are given by $x_r(l), x_r'(l)$ where l is a distance from the object point. Note that the shape function F(s), describing lenses surfaces, is placed now orthogonally to rays propagation (compare with [1]).

The most natural and simple construction of optimization criterion to minimize spherical aberrations ("SA") is a minimum of rms dimensionless deviation in the image point:

$$\Phi_{SA}(\mathrm{F}) = \left\{ \frac{1}{N^{rays}} \sum_{r=1}^{N^{rays}} \frac{x_r^2(\mathbf{L}^{image})}{X_a^2} \right\}^{1/2} \to \min \tag{7}$$

where the divisor X_a^2 stands for the square of lens aperture and is used for normalization. The minimal possible value of Φ_{SA} is obviously zero, that corresponds to ideal focusing without dilution.

The boundary conditions now can be written as

$$\left\{ \begin{array}{llll} \mathrm{F}(\tilde{\mathrm{s}}_0, l_1) & = \mathcal{F}_0(l_1) & \mathrm{F}(\tilde{\mathrm{s}}_1, l_1) & = \mathcal{F}_1(l_1) \\ \mathrm{F}'(\tilde{\mathrm{s}}_0, l_1) & = \mathcal{F}_0'(l_1) & \mathrm{F}'(\tilde{\mathrm{s}}_1, l_1) & = \mathcal{F}_1'(l_1) \\ \mathrm{F}(\tilde{\mathrm{s}}_0, l_2) & = \mathcal{F}_0(l_2) & \mathrm{F}(\tilde{\mathrm{s}}_1, l_2) & = \mathcal{F}_1(l_2) \\ \mathrm{F}'(\tilde{\mathrm{s}}_0, l_2) & = \mathcal{F}_0'(l_2) & \mathrm{F}'(\tilde{\mathrm{s}}_1, l_2) & = \mathcal{F}_1'(l_2) \\ & \vdots & & \vdots \\ \mathrm{F}(\tilde{\mathrm{s}}_0, l_P) & = \mathcal{F}_0(l_P) & \mathrm{F}(\tilde{\mathrm{s}}_1, l_P) & = \mathcal{F}_1(l_P) \\ \mathrm{F}'(\tilde{\mathrm{s}}_0, l_P) & = \mathcal{F}_0'(l_P) & \mathrm{F}'(\tilde{\mathrm{s}}_1, l_P) & = \mathcal{F}_1'(l_P) \end{array} \right. \tag{8}$$

where $1 \le p \le P$ and "P" now denotes the number of lenses used (our program has no limitations on "P", but usually the number of glass lenses hardly exceeds 8–10).

Since the calculation of the criterion (7) is based on a straightforward ray tracing the optimization procedure operates pretty fast and the aspherical surfaces, corresponding to the minimum of Φ_{SA} were found within few seconds (for $N^{rays} = 40$, using PC with CPU 200 MHz). The unknown boundary parameters $\mathcal{F}_0(l_p)$, $\mathcal{F}_1(l_p)$, $\mathcal{F}_0'(l_p)$, $\mathcal{F}_1'(l_p)$ were found also numerically, as it was described above in section 2.

Fig. 2 shows the shape function $\mathrm{F}_{asph1}(s)$, corresponding to the optimized aspherical lens which ensures the fine focusing both for paraxial and non-paraxial beams, as demonstrated in Fig. 3. We assume that the object distance is $\mathbf{L}^{object} = -100$ mm, the image

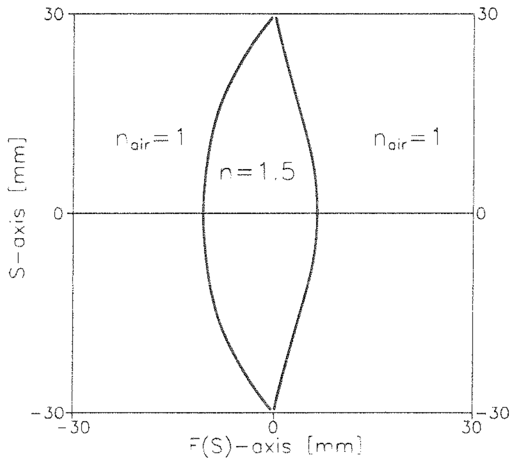

Figure 2: Shape functions $F_{asph1}(s)$. Refraction factor is equal 3/2.

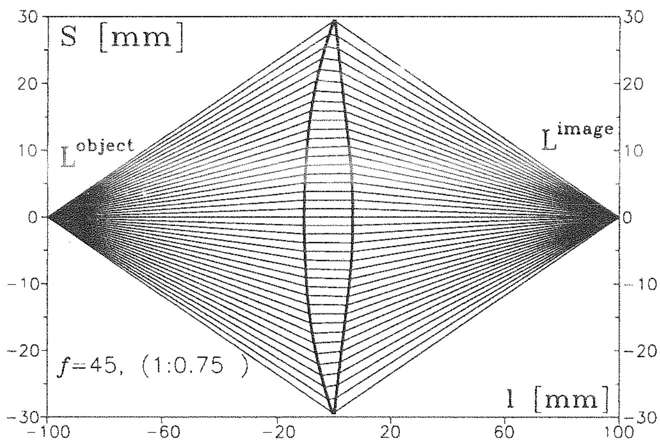

Figure 3: The optimized aspherical lens with the shape function $F_{asph1}(s)$ and the relative aperture is of $\emptyset : f$=1:0.75, providing a fine focusing for full aperture beams.

distance is $\mathbf{L}^{image}$ = 100 mm and $\emptyset$=60 mm; the principal focus is equal f=45 mm (found numerically, since the analytical formula (6) is not valid anymore). As a result, the aperture ratio is of $\emptyset : f$ =1:0.75, that is even more extreme, than for the considered above spherical lens.

Note, that here and below we are not using an analytical power expansion to represent aberrations, but perform a straightforward ray tracing. It means, that the found lens actually eliminates 3-rd, 5-th and higher order aberrations for extreme magnitude of the aperture ratio. This is a very good practical result.

The optimization can be performed for different object and image distances (even for $\mathbf{L}^{object} = \infty$ or $\mathbf{L}^{image} = \infty$) and for various combinations of constraints, as shown further. In particular, the aspherical lens can be symmetric, that sometimes may be useful as well.

Distortion. The next question which arises after suppressing the spherical aberration is a minimization of distortion. If the object has a height h^{object} and the image has corre-

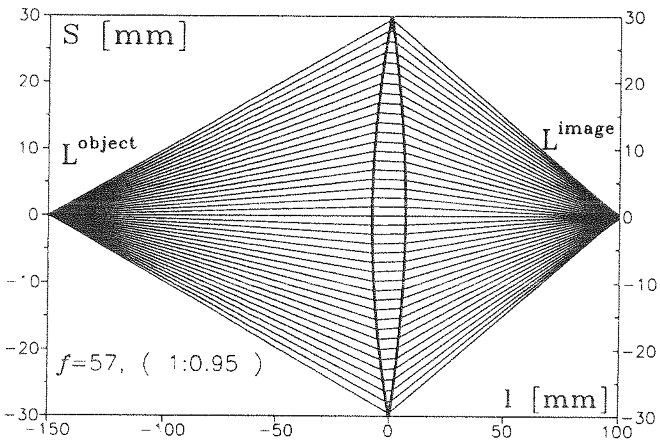

Figure 4: The optimized aspherical lens with the shape function $F_{asph2}(s)$ and the relative aperture is $\emptyset : f$=1:0.95, providing a fine focusing for full aperture beams.

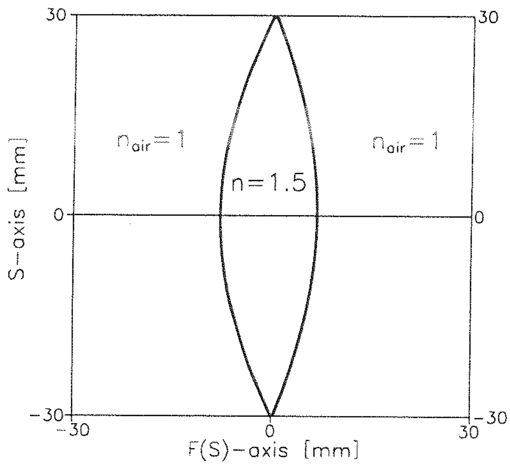

Figure 5: Shape function $F_{asph2}(s)$. Refraction factor is equal 3/2.

spondingly h^{image}, then the presence of distortion means a changing of the magnification factor $\mathcal{K}$ for different "h" magnitudes.

$$\mathcal{K}(\mathrm{F}) = \frac{h^{object}}{h^{image}}$$

The distortion will be absent when $\mathcal{K}(\mathrm{F}) \equiv const.$ The suppression of distortion is important when we wish to obtain the true image picture for the full aperture.

Obviously, the criterion Φ should include an additional "distortion term":

$$\Phi(\mathrm{F}) = \Phi_{SA} + \Phi_{Dist} \rightarrow \min$$

where $\Phi_{Dist} = d\mathcal{K}/dh$ (obviously, for $\Phi_{Dist}(\mathrm{F}) = 0$ we have no distortion at all).

It was shown in [5], how an optimized lens manages spherical aberration combined with distortion, using the full aperture.

Coma. The coma arises when the object points are off-axis. To reduce this aberration, the "Abbe criterion" should be satisfied (see for more details [2, 8, 11]), so our algorithm should additionally minimize the "coma term":

$$\Phi_{Coma}(\mathrm{F}) = \left\{ \frac{1}{N^{rays}} \sum_{r=1}^{N^{rays}} \left[\left| \frac{\sin(x_r'(\mathbf{L}^{object}))}{\sin(x_r'(\mathbf{L}^{image}))} \right| - \mathcal{K} \right]^2 \right\}^{1/2}$$

where $\mathcal{K}$ is a factor of magnification. The found above function F_{asph2} provides both focusing regimes in Figs. 4,6. This solution is rather important for practical light optics design.

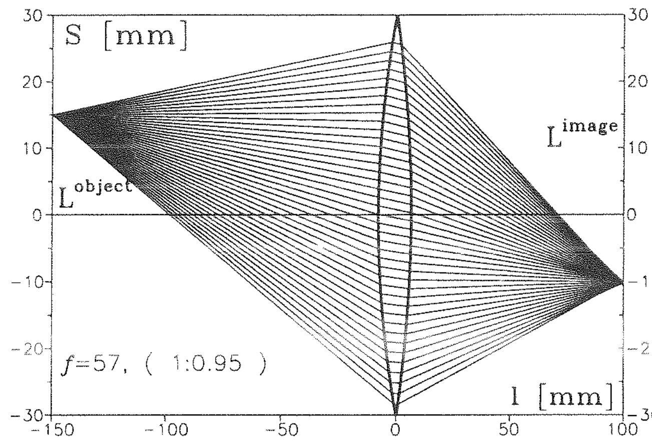

Figure 6: Non-paraxial oblique rays through the optimized aspherical lens with the same shape function $\mathrm{F}_{asph2}(s)$. The coma is minimized.

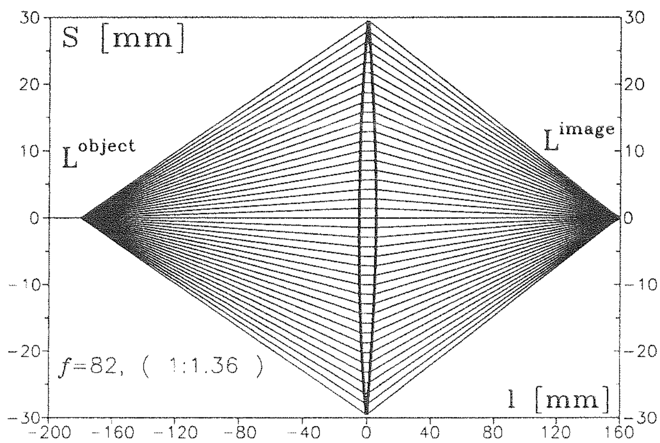

Figure 7: The aspherical lens with the shape function $\mathrm{F}_{chrom}(s)$, optimized for non-paraxial monochromatic rays.

Chromatic aberration (Dispersion). Now we take into accont a composite structure of white light. Since rays with different colors have different refraction factors, they will

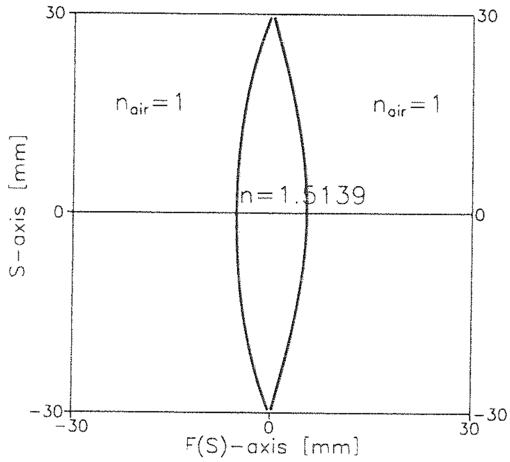

Figure 8: The shape function $F_{chrom}(s)$.

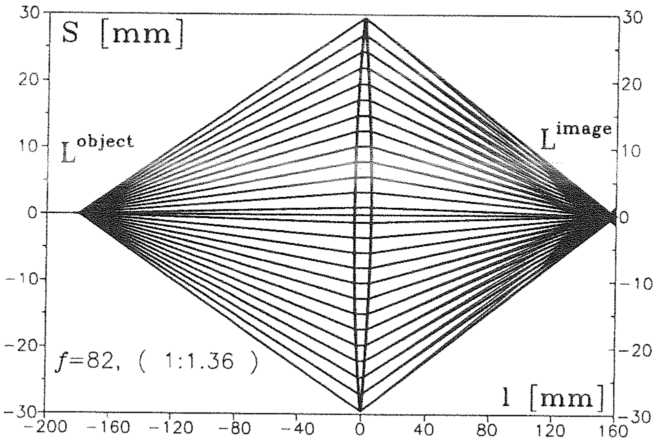

Figure 9: Illustration of chromatic aberration: non-paraxial rays (3 colours: red, green, violet) through the lens with the shape function $F_{chrom}(s)$.

have different focusing lengths; this results in image dilution. So, originally fine focusing from the Figs. 7, 8 will be spoiled by these effects, as shown in the Fig. 9: one can distinguish the split of the original white light by three fractions (this phenomenon is especially demonstrative on a colour monitor). The dilution of the focusing spot due to achromatism can be partly reduced, however can not be eliminated only by one lens.

As is well known, a combination of few lenses, made from different kinds of glasses, can correct these chromatic aberrations. We give an example of apochromatic (i.e. achromatic for three colors: red, green and violet) system of 2 lenses, as demonstrated in Fig. 10. The found optimized objective consists of two glued glass lenses: focusing and defocusing.

- The refraction indices of the focusing lens (crown glass) were taken as the following: $n_{A'}$=1.5139 (for red Fraunhofer line), n_D=1.5163 (for yellow-green Fraunhofer lines), $n_{G'}$=1.5262 (for violet Fraunhofer line).

- The refraction indices of the defocusing lens (flint glass) were taken, as $n_{A'}$=1.6421 (red), n_D=1.6477 (yellow-green), $n_{G'}$=1.6725 (violet).

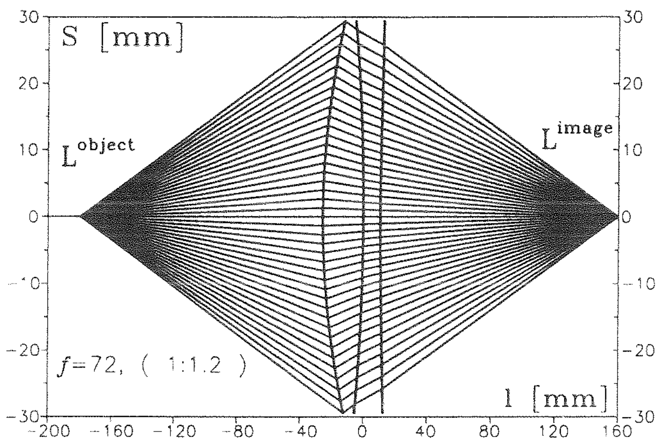

Figure 10: Optimized apochromatic objective with the shape function $F_{achr}(s)$ and the relative aperture is $\emptyset : f$=1:1.2. Two lenses with different refraction factors are used: the focusing lens is made from the crown glass and the defocusing — from the flint glass. Three colors: red, green and violet have a common sharp focus for full aperture beams.

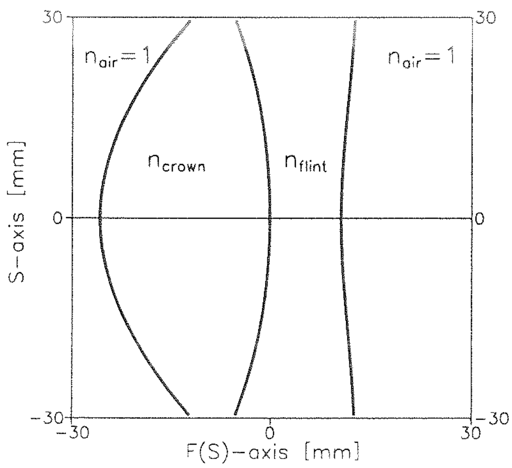

Figure 11: The apochromat shape function $F_{achr}(s)$ of two glued lenses.

The found solution is very useful, since has a very big relative ratio of $\emptyset : f$=1:1.2 for the whole spectra of visible light and consists only from two glued lenses.

The construction of the achromatic term can be similar to (7), computed for corresponding colors. Note, that together with visible part of the light, one can optimize also infrared and/or ultra violet spectra, that can be important for cameras and telescopes.

As a result, the functional, which estimates the quality of focusing, will have such a form

$$\Phi_{Aspherical}(F) = \Phi_{SA}(F) + \Phi_{Dist} + \Phi_{Coma}(F) + \Phi_{Achr}(F) \rightarrow \min \qquad (9)$$

which allows to design universal aspherical lenses.

4 Discussion and Conclusion

There are some other imperfections, such as astigmatism, field curvature. Their elimination assumes additional terms in the general criterion of optimization (9). Sometimes the requirements of ideal focusing are contradictory and the absolute minimum of the composite functional (9) can be hardly achieved. In practice, therefore, the optimization of optical objectives can be partial, assuming the specific purposes of the applications and maintaining a reasonable balance of aberrations. This may be managed by weight factors.

For general functional (9), we will be not able perhaps to design high-perfomance aspherical lenses with very big relative ratio (e.g. with such an extreme value $\emptyset : f=1:0.75$, as in the examples above), however our method will always lead to best possible solutions.

As it was mentioned above, there is a well-known family of analytical aspherical surfaces (see [2]) which correct the aberrations. We want to emphasize that the aspherical surfaces, found numerically by our method, represent a much more general set than second order analytical functions (e.g. hyperbolical, elliptical, etc.) and our algorith is able to approximate very special shape functions.

Finally, the construction of the general optimization criterion Φ may also include the economical factors: size, weight and cost.

Numerical experiments have demonstrated an effectiveness and a flexibility of the algorithm for RFQ matching sections optimization [1, 6] and for high-performance aspherical lenses design. Currently we have good preliminary results on time-of-flight (TOF) mass spectrometers synchronization, which allow to upgrade drastically the resolution factor of the ions with a very big energy spread by a proper shaping of the potential of the repeller field [12]. We have therefore a confidence to recommend our algorithm for other practical applications, when a performance may be improved via a proper shaping.

Acknowledgements

A part of this work was done when one of the authors (L.G.V.) stayed at II. Physikalisches Institut, Universität Gießen. He takes the opportunity to thank Prof. Wollnik and the staffs for their hospitality extended to him. He also thanks Drs. A.Kalimov (SPTU, St.Petersburg), M.Yavor (IAI St.Petersburg, RAS), V.Raznikov and V.Zelenov (BINEP Chernogolovka, RAS) for valuable suggestions and comments.

References

[1] L.G. Vorobiev and R.W. Müller, GSI-96-06 Report, Darmstadt (1996).

[2] L.C. Martin: Technical Optics, vol. **2**, Sir Isaac Pitman & Sons, London.

[3] M.M. Rusinov: Aspherical surfaces in optics, 2-nd edition, Moscow (1973).

[4] G.A. Korn and T.M. Korn: "Mathematical Handbook", McGraw-Hill (1968).

[5] L.G. Vorobiev: Preprint ITEP-16, Moscow (1997).

[6] D.G. Koshkarev and L.G. Vorobiev: NIMA, **336** (1993), 291-300.

[7] W.H. Press, B.P. Flannery, S.A. Teukolsky, W.T. Vetterling: "Numerical Recipes", Cambridge (1991).

[8] G.G. Slusarev: Methods for optical systems design, 2-nd edition, Leningrad (1969).

[9] V.V. Gorelic: Fabrication of aspherical lenses, Moscow (1978).

[10] Ch. Huygens: Traité de la Lumière, Leiden (1690).

[11] M. Born and E. Wolf: Principles of Optics, Pergamon (1968).

[12] L.G. Vorobiev and R.W. Müller, to be published.